Cold bending of vertical glass plates: wind loads and geometrical instabilities

Authors

Virginio Quaglini[(a)] ; Sara Cattaneo[(a)] ; Carlo Pettorruso[(a)] ; Luigi Biolzi[(a)]

Affiliation:

[(a)] Politecnico di Milano, Department of Architecture, Built Environment and Construction Engineering, Piazza Leonardo da Vinci 32, 20133 Milan, Italy;

e-mail address:

virginio.quaglini@polimi.it ; sara.cattaneo@polimi.it ; carlo.pettorruso@polimi.it ; luigi.biolzi@polimi.it

Corresponding Author

Virginio Quaglini, MSc, PhD

Politecnico di Milano, Department of Architecture, Built Environment and Construction Engineering, Piazza Leonardo da Vinci 32, 20133 Milan, Italy

e-mail: virginio.quaglini@polimi.it

Abstract

The study investigates the mechanical response of glass shells cold bent into hyperparaboloid shapes used in building technology. Focus is addressed on two subjects: the application of the cold bending procedure to vertically oriented rather than horizontal glass plates, which allows to minimize the disturbance produced by the initial deflection due to the self-weight of the pane, and the effect of wind load on curved glass panels installed in glazing façades.

The particular case of a vertical monolithic glass plate (2000 × 2000 × 10 mm) loaded symmetrically on two diagonally opposite corners is studied experimentally and numerically, developing a finite element model, and the results compared each other. Both experiments and numerical analyses show that a mechanical disturbance, introduced e.g., on the centre of the plate, promotes a change in the deformation mode during the bending process. Geometrical instabilities which impair the optical quality of the glass, and trigger a serviceability limit state failure, are evidenced.

A parametric analysis is conducted to investigate the influence of the size and the aspect ratio of the glass plate on the cold forming procedure. The examined response parameters include the geometrical distortion of the glass plate, involving the possible occurrence of optical distortion and the maximum tensile stress in the plate.

In the second part of the study, the effect of wind load on curved glass shells is numerically evaluated. The results point out the possible trigger of a limit equilibrium stability, with a “snap-through” transition from an equilibrium state to another non-adjacent equilibrium configuration which can result in a sudden break of the glass plate. This phenomenon is affected from the size of the glass plate and the curvature imposed to the plate during cold bending. The proposed methodology could represent a convenient tool to assist practitioners in selecting the appropriate thickness of façade glass panels.

Keywords

Cold bending ; Curved glass ; Vertical plates ; Geometrical instabilities ; Equilibrium bifurcation ; Snap-through buckling ; Wind action ; Anticlastic shape

1. Introduction

Curved glass has been used for building purposes since the early nineteenth century, yet it has far from exhausted its potential, and its use is steadily increasing in contemporary architecture. In the context of the so called “fluid design”, fostered by the development of computer aided design technologies in the past twenty years, the use of curved glass has been more than ever favoured, since it facilitates the creation of unique free-form surfaces that are characterized by a combination of aesthetic appeal, transparency and use of natural light within buildings [1]. Typical uses include both interior and exterior applications, such as façades and display windows, skylights and cupolas, skywalks, entrances, revolving doors, canopies, winter gardens and conservatories, railings for staircases and elevated walkways, elevators, and partitions.

There are two main technologies for production of curved glass shells, depending on whether heat is involved in the process: hot bending and cold bending. Hot bent glass is obtained by heating glass sheets above glass transition temperature (600°C), and curving them into the desired shape using moulds. Then the panel is cooled down in a controlled manner, resulting in a tension free end product. Both single-and double-curvature surfaces can be obtained, but a major limit is represented by the need of a negative form: when using this method to produce many different façade panels, as one has to do for a free form design, equally many different moulds have to be set up. In recent years, numerically-controlled rolling machines have been developed that allow to obtain hot-bent glass sheets with single or even with small bi-directional curvature, and radius that varies in a continuous manner, without a mould. However, hot bending technologies are neither energy nor cost effective. Curved panels are indeed prepared at the factory, thereby requiring long delivery time and high transport costs to carry panels with different curvatures. Additionally, the optical quality of hot formed shells may be sometimes unsatisfactory. The thickness of the glass sheet can be locally affected from imperfections in the mould or from straightness and distortion of the rollers, resulting in optical distortions and reflections. To conclude, hot bending techniques fit for small projects with strong curvature, but large-scale projects need other techniques [2-6].

An alternative, energy- and cost-efficient method to produce curved glass panels is cold bending, in which elastic deformation of glass is induced at ambient temperature by applying out-of-plane loads. The process starts by fixing the flat glass unit to a frame that mechanically bends it into the desired shape. The frame is then ready for installation into the building. The process can be performed after the glass has been tempered, therefore allowing for enhanced mechanical properties of the end product. The bending radius is normally quite high, and the thinner the glass, the lower it is the required force to bend. Moreover, cold bending can be executed on site with a relatively small amount of equipment, and without any requirements for moulds, which reduces the costs and makes this an attractive technique for creating curved glass surfaces. Eventually, the surface appearance is very smooth as it is not affected by distortions created by the mould or the rollers. For shaped glazing units having a shallow curvature, cold bent glass is therefore more and more used instead of hot formed glass panels. Another recent technique is cold lamination bending [7], in which unbonded glass sheets and adhesive interlayers are firstly bent in the desired shape, and then laminated in autoclave. The interlayer preserves the curved shape of the glass in place, though a certain springback is triggered when the restraints are removed after lamination [8, 9]. One of the advantages of using this process is the possibility of making very flexible shapes, though at a higher cost than simple cold bending. Remarkably, application of the cold bending technology is today not limited to glass, but it is used as well for composite plates used in aerospace, civil, marine and other fields [10-14].

However, cold bending has also some limitations. Since the flat sheet is deformed elastically, permanent stresses are induced inside unit. The maximum curvature that can be achieved is limited by the maximum elastic stresses that can be safely resisted by the glass panel, accounting for both the stress produced during the forming and the stress induced by service loads. Therefore, toughened glass in the form of heat treated (heat strengthened or fully tempered) or chemically toughened glass is typically used. Also, there can be some relaxation in the glass over its lifetime, which can cause it to change its shape over time.

Cold bending can be used to create either single or double curved glass surfaces. Single (cylindrical) curved surfaces are easier to form, but double curved surfaces are more popular in architectural design as they provide more freedom and the possibility to create free-form façades. Double curved surfaces are defined by two radii of curvature and can be divided in synclastic and anticlastic surfaces. In synclastic surfaces (e.g., paraboloid geometry), both centres of curvature lie on the same side of the surface, while in anticlastic surfaces (e.g., hyperparaboloid geometry) the centres of curvature lie on different sides. Depending on the pane dimension and shape, synclastic and anticlastic shapes can be produced having radii from 17 to 40 m, and spans up to 9 – 14 m [15]. Some of the most notable examples of application of cold bent double curved glass shells are e.g., the TGV railway station in Strasbourg [2], the glass roof for the medieval and renaissance gallery of the Victoria and Albert Museum, London [16], the Ocean Heights Tower in Dubai and the IAC Headquarters in New York [17].

The internal stress is not the only mechanical factor that limits the maximum curvature that can be achieved with cold bending. Geometrical instabilities can indeed occur during the warping of the glass sheet. Such phenomenon was firstly reported by Staaks and Eekhout [18-21], who considered square plates fixed at three corners, while the fourth corner was forced out-of-plane. This load condition results in a hyperparaboloid form of the plate, where both diagonals are curved, and the edges remain straight. However, when the displacement at the forced corner reaches a certain value, namely 16.8 times the thickness of the sheet [18], a noticeable change in the deformation mode is triggered, as one of the diagonals tends to straighten, while the second diagonal becomes more curved. This kind of buckling, in which the geometry of the plate changes from an anticlastic double curved to an approximatively single curved shape, has been observed in a number of experimental and numerical works published in the last years, accounting for multiple panel sizes and aspect ratios, and different boundary conditions [7, 8, 17, 20-30].Notably, this change in the deformation mode is accompanied by two phenomena: (a) the edges of the plate, which remain straight in the early stage of bending, become curved; and (b) local instability appears on the stiffened diagonal in form of

ripples [25]. Curved edges endanger the assembly of glass panes as they make it difficult to fix the plate to a frame and/or to align the edges of adjacent plates. The ripples observed in cold bending (generally referred to as cold bending distortion) can impair the optical quality of glass by producing optical distortion and therefore trigger a serviceability limit state failure. In accordance with the provision of the European standard EN 12150-1 [31] that limits the amplitude of roller wave distortion in fully toughened glass to 0.5 mm over a length of 300 mm, some authors [32-33] recommend to apply the same limit to cold bending distortion in order to determine whether the optical quality of the curved plate is acceptable.

The instability may be triggered from several factors, including the plate orientation and the support conditions. A first distinction can be made indeed between glass plates linearly supported along the edges and glass plates restrained at some points [17]. The situation of horizontally oriented plates supported at two diagonally opposite corners was extensively investigated by Datsiou [25-26], who concluded that in this condition it is the forced diagonal that, once buckling is triggered, acquires more curvature, while the curvature of the other diagonal diminishes. Another remarkable finding is that this change of deformation mode occurs gradually with increasing load, whereas a snap-through instability in the form of a sudden reversal of the direction of curvature of the diagonal is triggered when the loaded corners are forced to displace in the direction contrary to the initial deflection of the plate resulting from e.g., its self-weight or surface imperfections [25-26].

Additional deformation and increased stress of curved glass panels occur because of the external loads the units in service are subjected to. In roof constructions, nearly all permanent (self-weight) and accidental (snow) loads act in the vertical direction, more or less perpendicular to the shell surface, thus generating bending stresses that build up to the stress produced during the cold shaping. In façade panels the gravity load is mostly supported by diaphragm action according to vertical load paths to the ground, but, on the other side, the panels may be exposed to wind blowing normal to the surface. Being wind a short term load, long term effects are avoided; however high wind pressure can induce large stresses in glass panes, as well as modify their curved shape resulting in optical distortion

of images and impaired aesthetic function [9, 34-35]. Extensive research on the effect of out-of-plane loading on innovative cold bent glass-steel hybrid cells for building skins was conducted in the framework of the European Research Fund for Coal and Steel project called “S+G” [27], and results of full-scale experimental tests, performed on horizontally oriented elements, were presented by Hoffmeister [36].

The study aims at providing a deeper insight into the subject by investigating the forms of instability triggered in point-supported vertical glass panels that are cold formed into an anticlastic shape. The first part of the paper involves a combined experimental and numerical study, considering a 2000 × 2000 mm monolithic glass sheet, and explores the effect of an out-of-plane perturbation on the deformation mode of the vertical plate. Methods and results are presented in Sections 2 and 3, respectively. In section 4, the validated numerical model is used to perform a parametric study and assess the influence of the dimensions and the aspect ratio of glass units on the trigger of global and local instabilities during the cold bending of originally flat plates. The effect of wind load on curved façade glazing is hence investigated in Section 5 through the execution of numerical analyses on curved glass panels subjected to the application of an out-of-plane load. Eventually, in Section 6 the main results and the findings of the study are summarized and discussed.

2.Methods

2.1 Experimental Investigation

The aim of the test was to assess physically the trigger of instability during the cold bending of a tempered glass panel arranged in vertical position.

A monolithic glass plate was examined. Monolithic cold bent glass is expected to also provide the base for future research on the more complicated subject of cold bent laminated glass [25]..Indeed, according to the Italian guideline CNR DT 210 [37] approximate methods, like e.g. the Wölfel-Bennison [38], or the Enhanced Effective Thickness (EET) method [39-41], can be used to evaluate the thickness of a monolithic glass with equivalent bending properties. The test specimen was a 2000 × 2000 × 10 mm thick fully tempered glass plate. The edges were polished before toughening in order to reduce the possibility of premature failure from edge flaws. Prior to testing, the residual stress on the surface of the plate was measured with a Strainoptics Laser Gasp Polarimeter according to EN 12150-2 [42]. Five spot readings were taken on either surface, and the mean residual compressive stress resulted as 106.5 MPa. Since the average tensile strength of float glass is on the order of 45 MPa, the resulting strength of tempered glass was about 150 MPa.

The load apparatus was arranged as shown in Fig. 1. The plate was held vertically in order to prevent the initial deflection of glass that occurs in horizontal panels as an effect of their own weight. The supports were two steel struts fixed to the reaction floor of the laboratory by ground anchors. The glass plate was restrained at two diagonally opposite corners (support points B and D, Fig. 1) by means of swivel joints type Sadev R1006 TSSA bonded to the plate through an adhesive. Out-of-plane displacements were imposed to the plate by means of two screws, pushing two aluminium plates glued on the two other corners of the plate (load points A and C, Fig. 1). The screws were hand-driven; however, the loading rate was deemed not to affect the geometric response of the monolithic glass [25].

Accounting for the size of brackets, support and load points were arranged symmetrically so that their centres were 67.5 mm away from the edges of the panel. Swivel joints at points B and D restrained translation in any direction, leaving rotational freedom to the plate. At points A and C the two screws allowed free rotation and in-plane translation.

Five LVDT transducers (Hottinger Baldwin Messtechnick GmbH, model WA100) with 100 mm capacity were used to measure the deflection of three points on each diagonal, including the centre of the plate (Fig. 2). The reaction forces at support points B and D were measured by two load cells (Hottinger Baldwin Messtechnick GmbH, model K-C10 25 kN) fixed to the struts.

Two experiments were performed. In the first experiment, a symmetric displacement $\delta_{AC,z}$ was imposed on points A and C and gradually increased in 10 mm steps up to 120 mm. At each increment, panel deflection and reaction forces at support points B and D were recorded. A change in the mechanical response of the plate, highlighting the possible trigger of a buckling condition, was observed at a corner displacement of approximately 80 mm (Fig. 4b). In the second experiment, a small disturbance was introduced by applying a point load perpendicularly to the middle plane of the plate. A 5 mm diameter plunger, horizontally oriented and pointing to the centre point of the glass plate, was placed at 30 mm far from the initially flat specimen. Since in the first stage of loading the deformed shape of the plate is symmetric and the deflection at the centre of the plate is one half of the prescribed corner displacement, as it will be shown in Section 3.1, contact between the plate centre and the plunger was engaged at an imposed displacement of 60 mm, i.e. before the stability limit for the undisturbed plate was reached. . The plunger was supported by a vertical cantilever rod provided with low stiffness (on the order of 2 kN/m), so that it could accommodate the horizontal displacement of the plate with a negligible reaction force. The total displacement $\delta_{AC,z}$ = 120 mm was imposed again on the load points A and C in 10 mm steps, and panel deflection and reaction forces recorded.

-

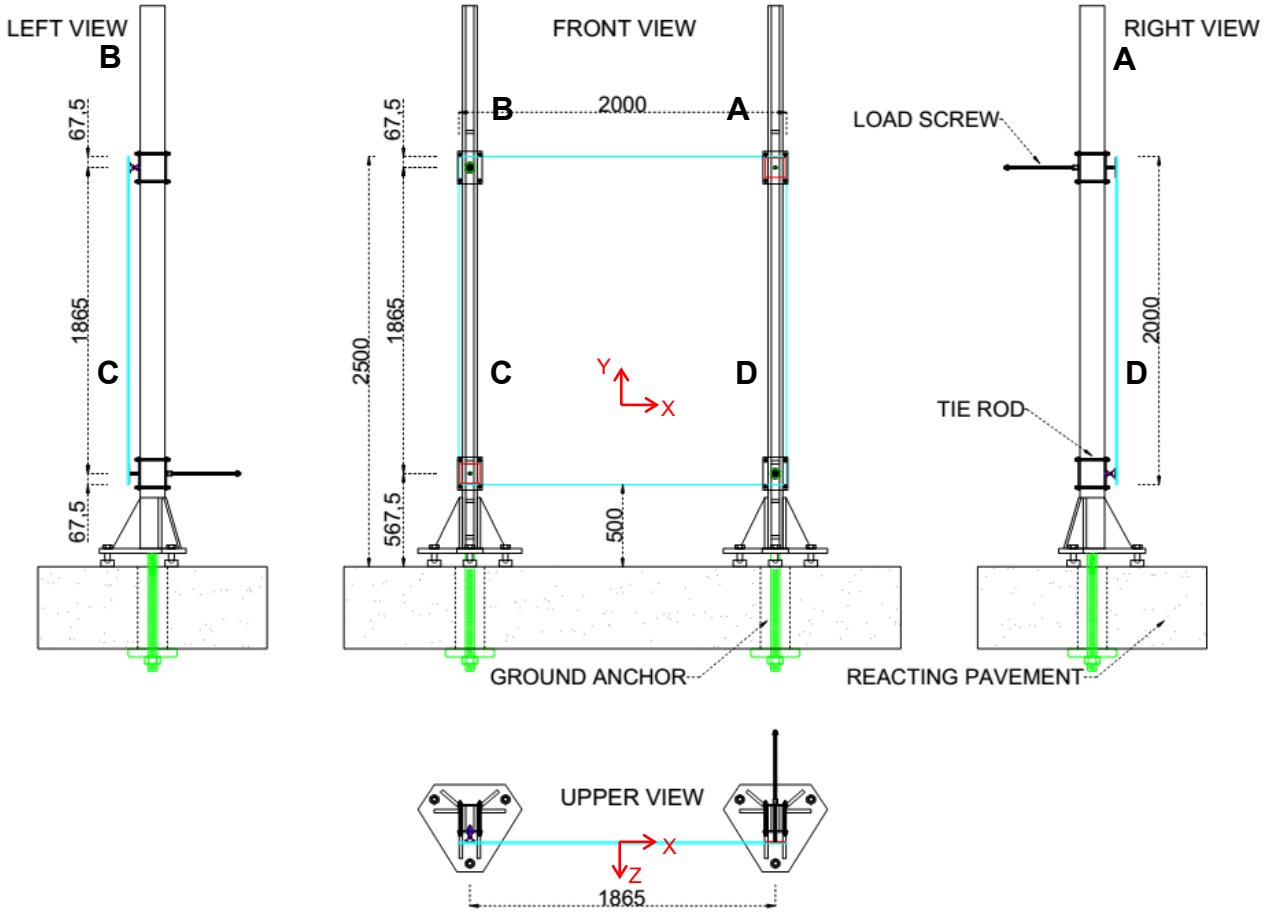

Fig. 1 – Test configuration

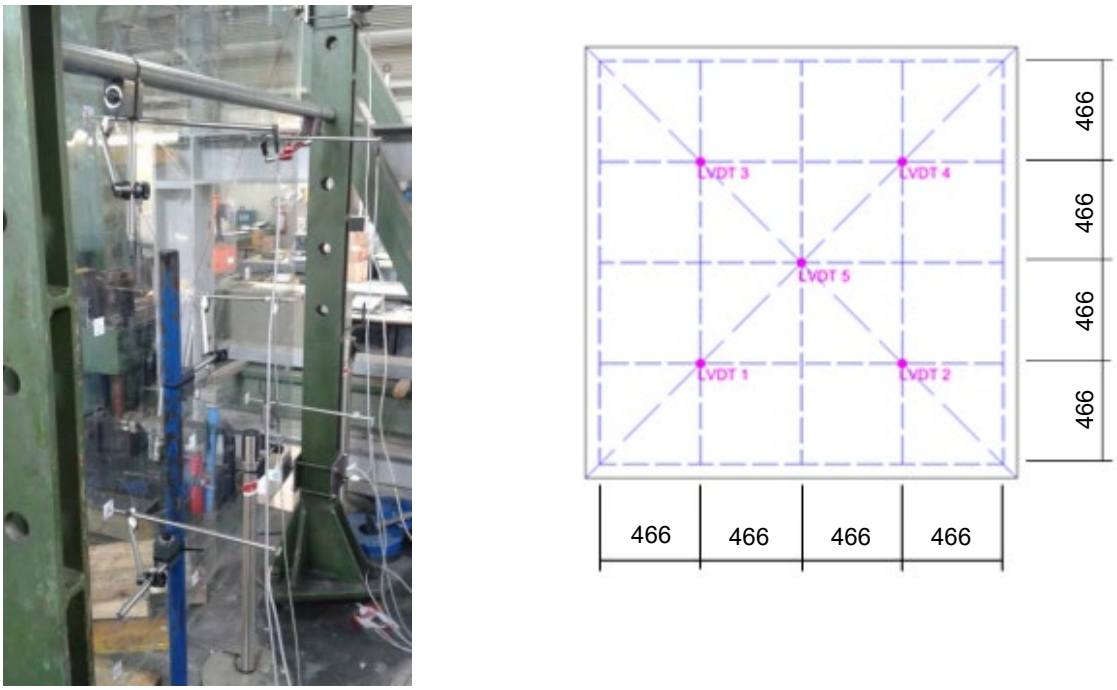

Fig. 2 – Position of LVDT displacement transducers (dimensions in mm)

2.2 Numerical Investigation

A finite element model of the tested glass plate was formulated within *Abaqus/CAE 2017* [43] using twenty-node quadratic brick elements with reduced integration, corresponding to the element type *C3D20R* [17, 25]. A linear behaviour was associated to glass, with Young modulus E = 70 GPa, and Poisson coefficient ν = 0.22. The 3D structural mesh of the plate was created by dividing the edge length in 20 elements and the thickness in 3 elements, resulting in an element size of 100x100x3.33 mm (length x length x thickness) (Fig. 3). Stress and displacement convergence tests were preliminarily performed to select the mesh density and provide a good balance between the solution accuracy and the computational cost.

The model considered the vertical panel, so that the self-weight of the glass was disregarded in the analyses due to its negligible flexural contribution. The plunger introduced in the second experiment was modelled as a 5 mm diameter cylinder made of steel (Young modulus E = 210 GPa and Poisson coefficient ν = 0.32) supported by a linear spring with stiffness K = 2 kN/m.

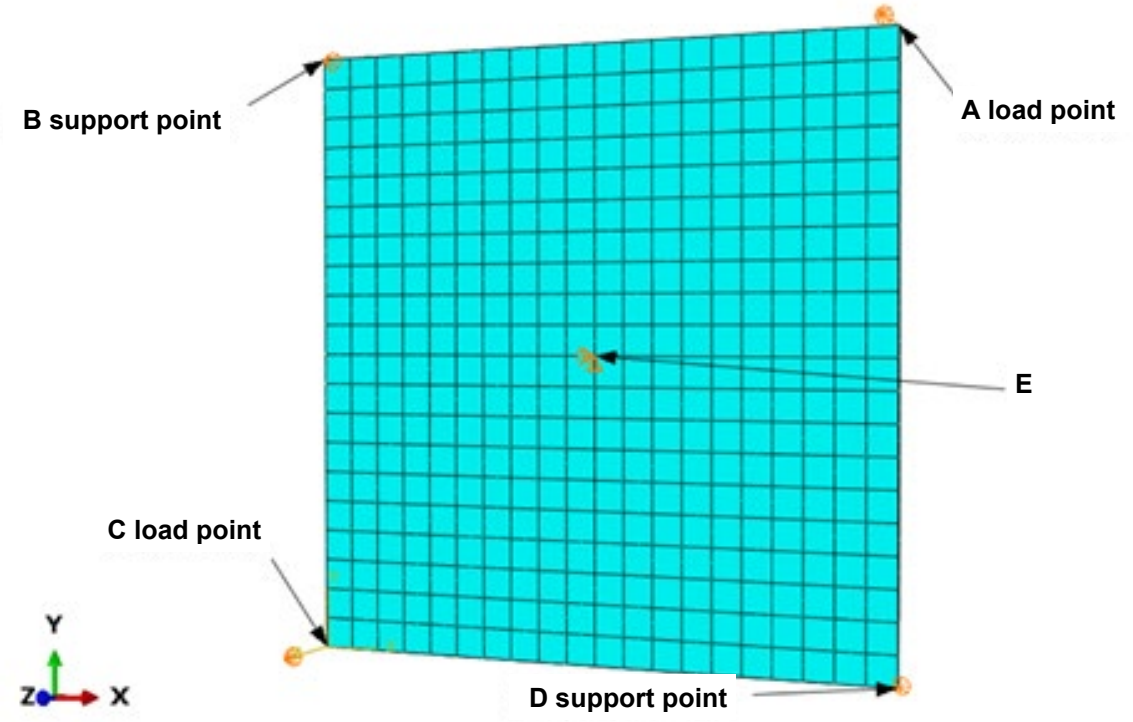

Fig. 3 – Four-point loaded glass plate. Numerical model of the loaded section bounded by points A, B, C, D

By referring to Fig. 3, in order to reproduce the boundary conditions implemented in the experiments, a symmetric displacement δ_z along the Z-axis was imposed on two corners (points A and C), while pinned supports, restraining translation but leaving rotation free, were modelled at the other two corners (support points B and D); to maintain the symmetry of the system, in-plane translations (i.e. along X and Y axes) of the centre point E of the plate were restrained. The two experiments described in Section 2.1 were numerically reproduced. The finite element calculation was performed using the static general analysis method coded in Abaqus in order to take into account the geometrical nonlinearity associated to the out-of-plane displacement of the plate. The analyses simulated a displacement-driven test, while the influence of the displacement rate on the mechanical properties of glass was disregarded [25].

3. Experimental and numerical results

Fig. 4a illustrates the deflection of the centre of the plate (point E in Fig. 3) versus the load P applied on each of the two corners A and C in either experiment (*Ver*: vertical plate without disturbance; *Ver*-disturbed: vertical plate with out-of-plane force opposing to the centre point displacement).

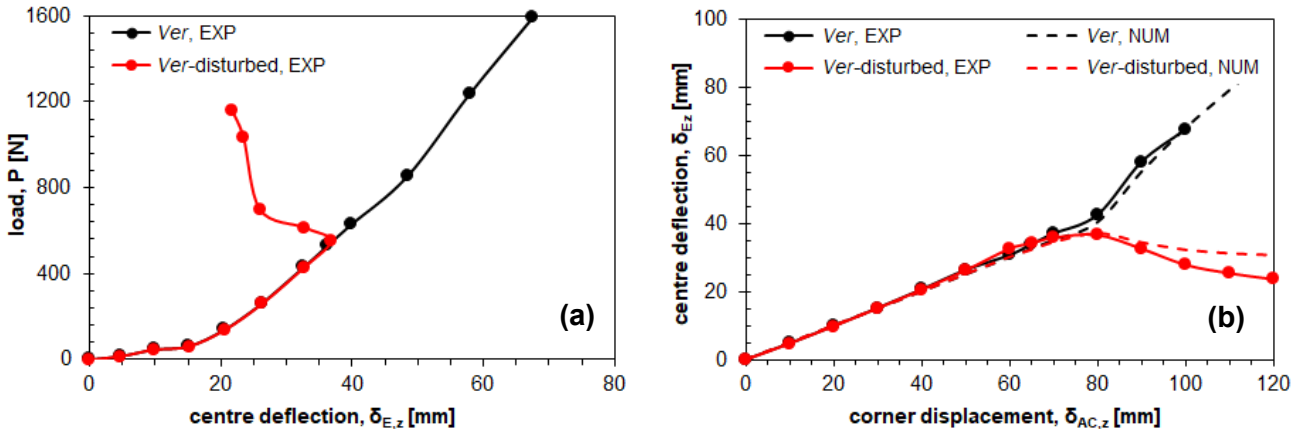

Fig. 4 – (a) Load P vs. centre deflection $\delta_{E,z}$; (b) centre deflection $\delta_{E,z}$ vs. imposed corner displacement $\delta_{AC,z}$ (experimental, EXP, and numerical, NUM, data)

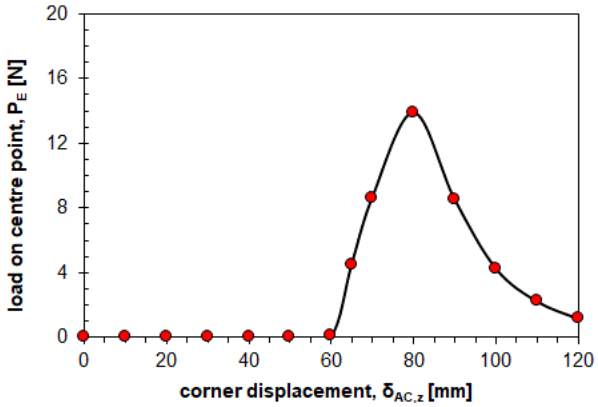

Fig. 5 – Load applied on the centre of the glass plate, P_E, vs.corner deflection $\delta_{AC,z}$ calculated in the numerical analysis

In the first experiment the P–$\delta_{E,z}$ relationship between force and displacement is monotonic and, when the early stage of deformation is disregarded, almost linear (Fig. 4a). The change in stiffness observed at $\delta_{E,z}$ = 15 mm is ascribed to geometrical effects due to the transition from small to large deflections [17].

In the second experiment in which a small disturbance is imposed at the centre of the plate, at a deflection $\delta_{E,z} \approx 40$ mm the monotonic P–$\delta_{E,z}$ relationship is broken, and a further increase in distortion fosters the centre of the plate to return gradually towards the original flat position. It must be underlined that the disturbance triggers the instability, but it does not provide any effect on the subsequent "post-critical" deformed shape, because as the deflection of point E diminishes, the perturbing force (which is produced by the elastic deflection of the cantilever rod supporting the plunger) declines as well (Fig. 5).

As shown in Fig. 4b the deflection of the centre of the plate increases linearly with the imposed corner displacement $\delta_{AC,z}$ at a rate $\delta_{E,z} \approx 0.5\ \delta_{AC,z}$ until approximately $\delta_{AC,z} \approx 80$ mm. Beyond this point, the deflection of the centre point of the undisturbed panel (*Ver*) continues to increase, though at a faster rate; in contrast, under the effect of the load perturbation the centre deflection declines (*Ver*-disturbed) as the corner displacement increases further. Numerical curves are also reported in Fig. 4b for comparison to the experimental data. The finite element formulation actually predicts a

response bifurcation at $\delta_{E,z}$ = 37.5 mm (i.e., $\delta_{AC,z}$ = 75 mm), which is very close to the observed behaviour. Notably, similar curves were recorded in reference [17], where the Authors pointed out a symmetric deformation of the plate along the two diagonal lines until a bifurcation point is reached; beyond this point one diagonal of the plate stiffens while the other takes most of the deformation. The same buckling instability has been indeed observed in the present study.

Fig. 6 and Fig. 7 display the deflection of the vertical plate along its two diagonal lines, calculated numerically with superimposed processed data from LVDT transducers, as function of the abscissa ξ on either diagonal. The change in the deformation mode is apparent from the analysis of the curvatures. Namely, in the first experiment (Fig. 6) at displacement $\delta_{AC,z} > 80$ mm the forced diagonal (dotted line) stiffens and becomes straight, and any increase in deformation is confined to the supported diagonal (continuous line). This behaviour results in the monotonic relationship between $\delta_{E,z}$ and $\delta_{AC,z}$ shown by curve in black (*Ver*) in Fig. 4b. The opposite behaviour is observed in the second experiment when a small perturbation is applied on the centre of the plate (Fig. 7). In this case, it's the supported diagonal that stiffens and straightens, and, hence, the central point deflection decreases.. This results in the decreasing curve in red (*Ver*-disturbed) in Fig. 4b. For both experiments the agreement between numerical and experimental data is satisfactory throughout the loading process.

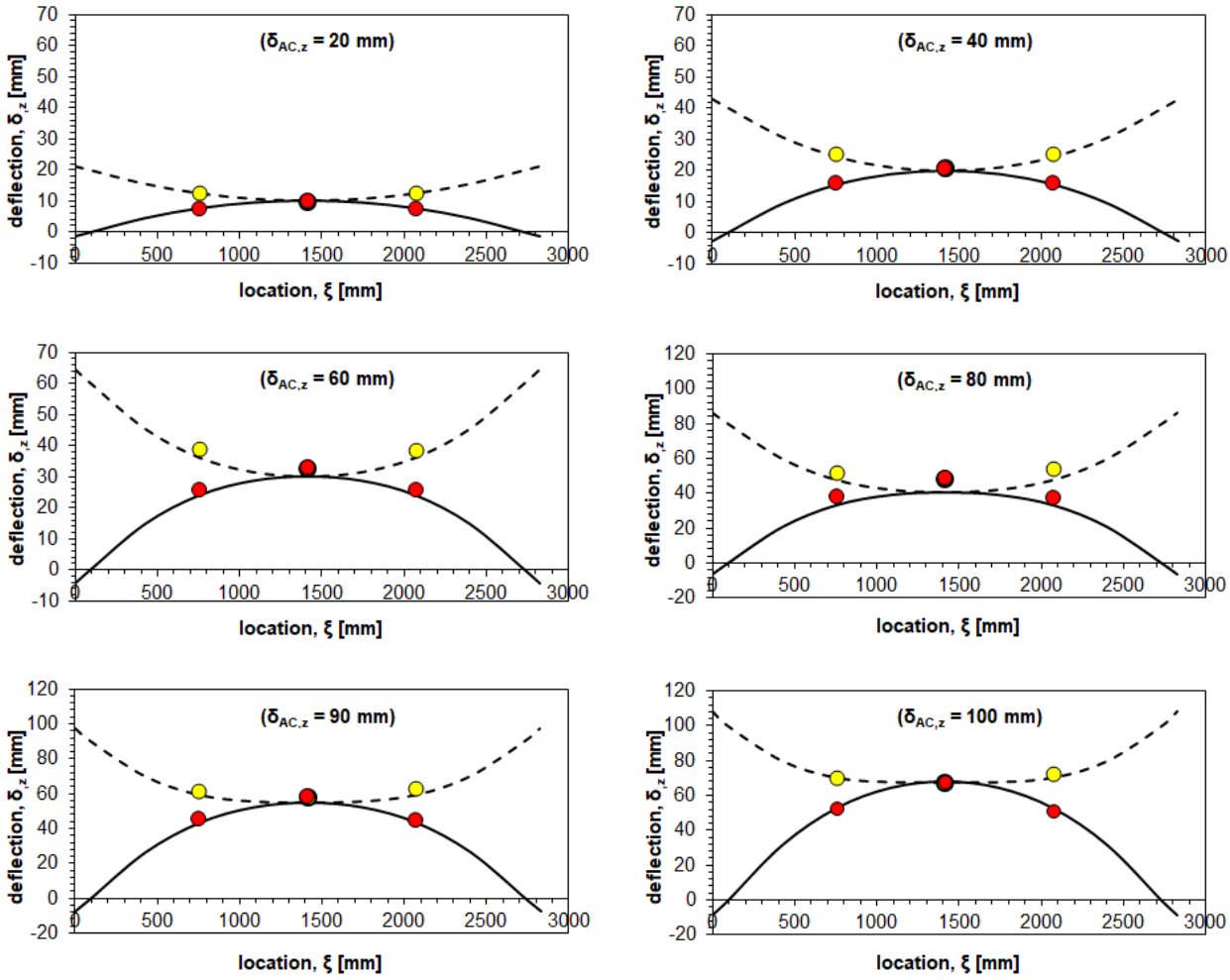

Fig. 6 – Superimposition of deflections along the forced (dashed) and the supported (continuous) diagonals. Numerical (lines) and experimental (dots) results for the glass plate without perturbation

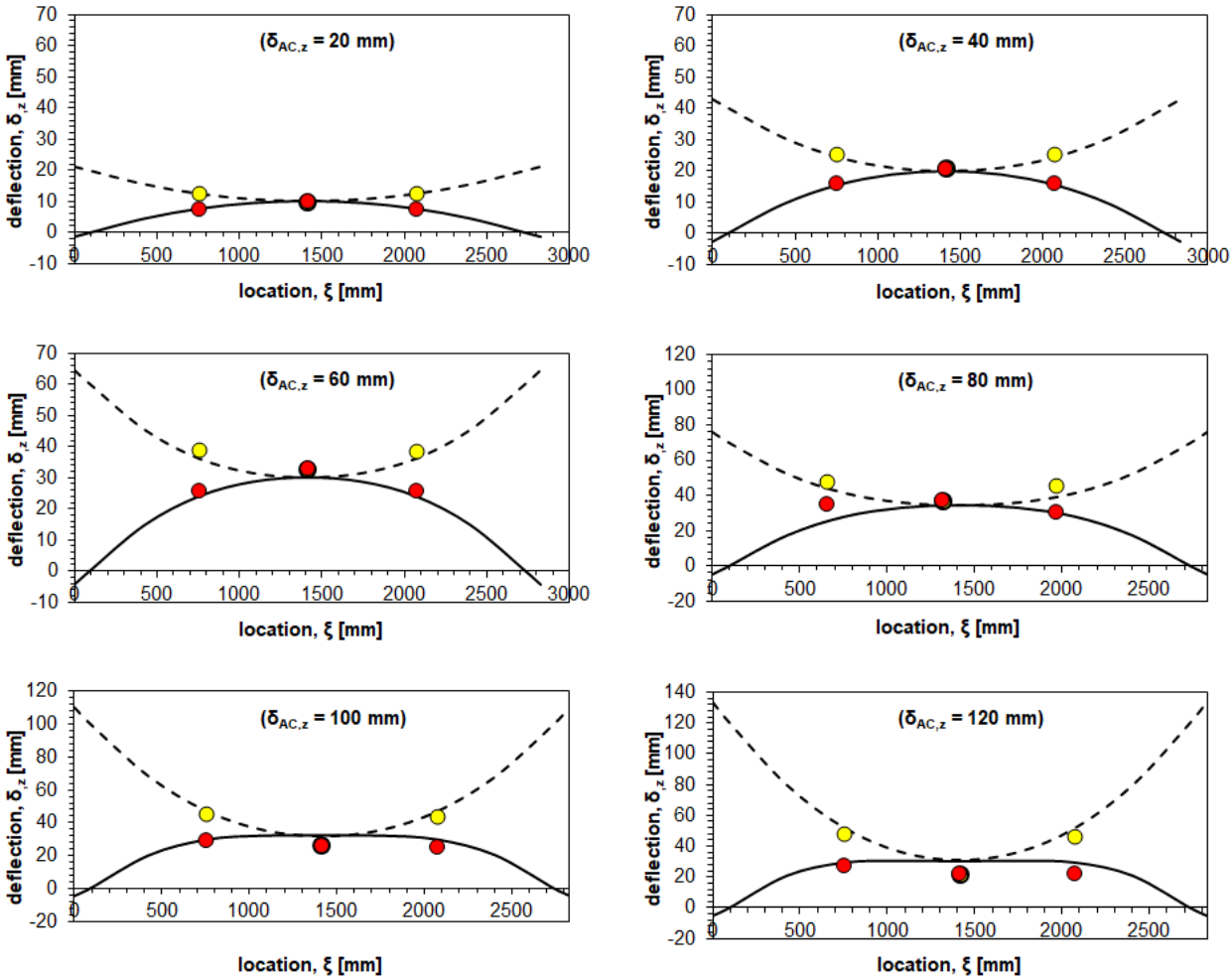

Fig. 7 – Superimposition of deflections along the forced (dashed) and the supported (continuous) diagonals. Numerical (lines) and experimental (dots) results for the glass plate subjected to a disturbance at the centre

The trigger of instability is more conveniently highlighted in Fig. 8, which displays the profiles of the two diagonals calculated at different corner displacement $\delta_{AC,z}$ in 20 mm steps. During the warping process, the plate acquires a double curved surface geometry, involving bending about two axes. At the early stage of the process the geometry of the curved surface is anticlastic and symmetric, i.e. the total deflection is accommodated in equal parts by the two diagonals (i.e., $\delta_{E,z} = 0.5\ \delta_{AC,z}$).

However, above a certain distortion of the plate, the symmetry between the deformed shapes of the two diagonals is disrupted. In the undisturbed plate, as $\delta_{AC,z}$ exceeds 80 mm, the forced diagonal gradually stiffens, and the further increase in deformation is almost entirely confined to the second diagonal (Fig. 8a and 8b). The stiffening of the first diagonal is accompanied by a local change in curvature in the middle part, which tends to become straight. Eventually, for very large displacements, e.g. $\delta_{AC,z} > 120$ mm, the curvature changes sign along the central third of the length of the forced diagonal, and the diagonal takes the shape of a two-trough ripple. The onset of ripples on one diagonal was already observed during cold warping of horizontal plates [25], and some authors [25, 32-33], in order to limit the consequent optical distortions, have recommended to restrict the amplitude of the geometrical distortion A_{dist}, i.e. the difference in height between the highest and the lowest points on the plate surface, to 0.5 mm over 300 mm length. In the present study on a 2000x2000x10 mm plate the, the limit value $A_{dist} = 0.5$ mm was actually exceeded at $\delta_{AC,z} = 130$ mm, while a maximum distortion amplitude of 0.84 mm was produced from an imposed displacement $\delta_{AC,z} = 150$ mm.

When the disturbance is introduced (Fig. 8c and 8d), the deformation mode changes from the one observed in the first test; the bending of the forced diagonal increases, while the curvature of the supported diagonal decreases as the centre of the plate returns towards its original flat position. It must be here recalled that the experimental setup was designed in order to introduce a perturbation suitable to pander the panel to its stability limit, but without forcing it beyond. Therefore, the change in the deformation mode is indeed an effect of the triggered instability of the panel. Similarly to the first experiment, for imposed displacements $\delta_{AC,z} > 120$ mm the curvature changes sign along the central third of the length of the stiffened diagonal, resulting in the creation of ripples. Interestingly,

the amplitude of the ripples is found to be independent on which diagonal stiffens, as the limit A_{dist} = 0.5 mm is reached again at about $\delta_{AC,z}$ = 130 mm..

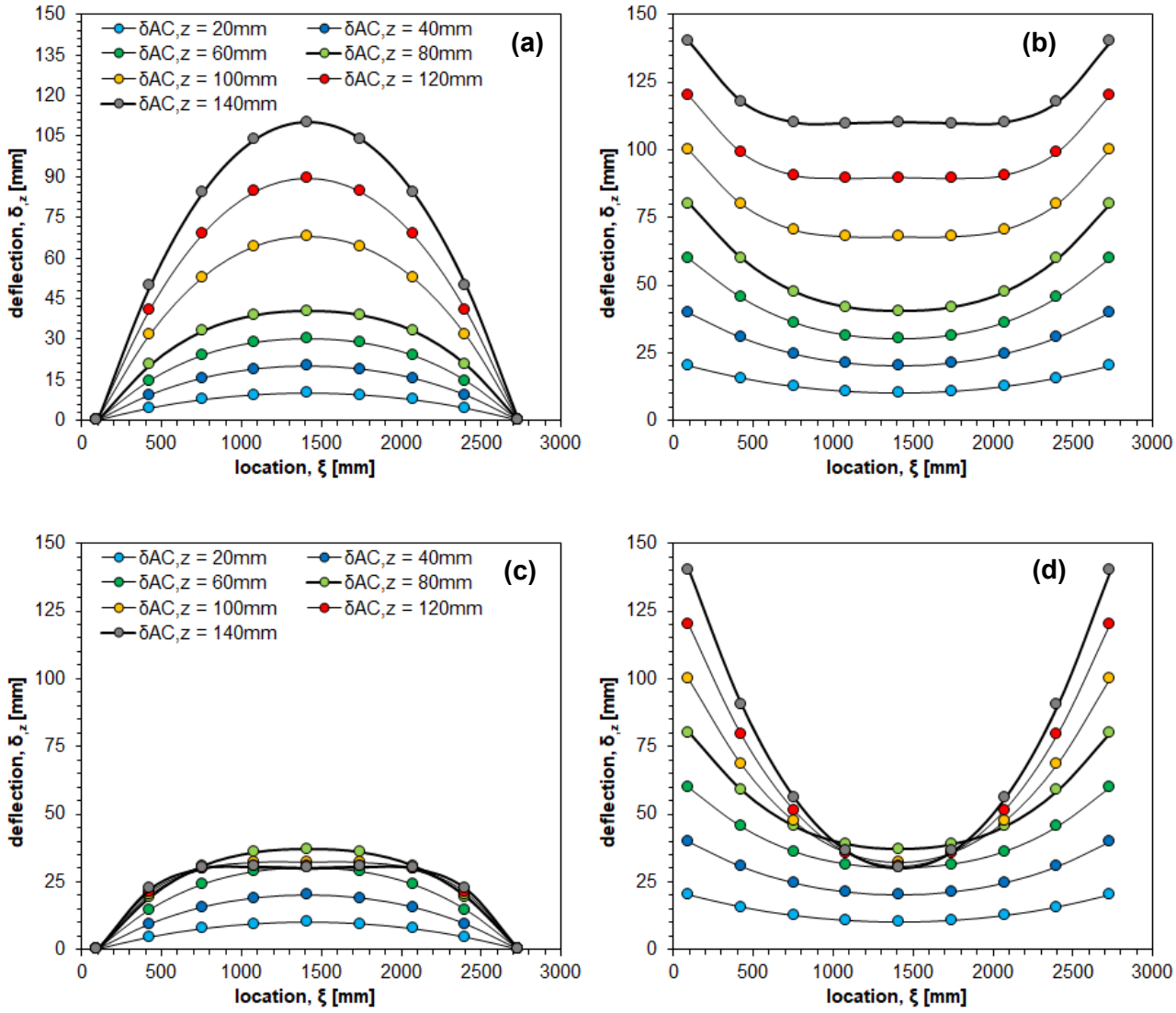

Fig. 8 –Supported and forced diagonal profiles at different prescribed displacements $\delta_{AC,z}$ for: (a) and (b) vertical glass plate without disturbance (*Ver*); (c) and (d) vertical glass plate with disturbance (*Ver*-disturbed)

In the early part of either experiment, for small deflections, the edges of the deflected plate remain straight (Fig. 9a). When the prescribed displacement increases at a point it cannot be considered small with respect to the plate size, geometrical nonlinearities come into place, and the deformed shape is still similar to a hyperbolic paraboloid but the edges tend to bow at their extremities. As highlighted by Galuppi et al. [17], this phenomenon may be regarded as a local instability, in which non-linear effects concentrate near the corners (Fig. 9b). Eventually, beyond the buckling limit of the plate, as a consequence of the stiffening of one diagonal, the central length of the stiffened diagonal becomes (more or less) straight and its whole deformation is confined close to the extremities (Fig. 9c and 9d). Therefore the edges of the deflected plate bend for all their length.

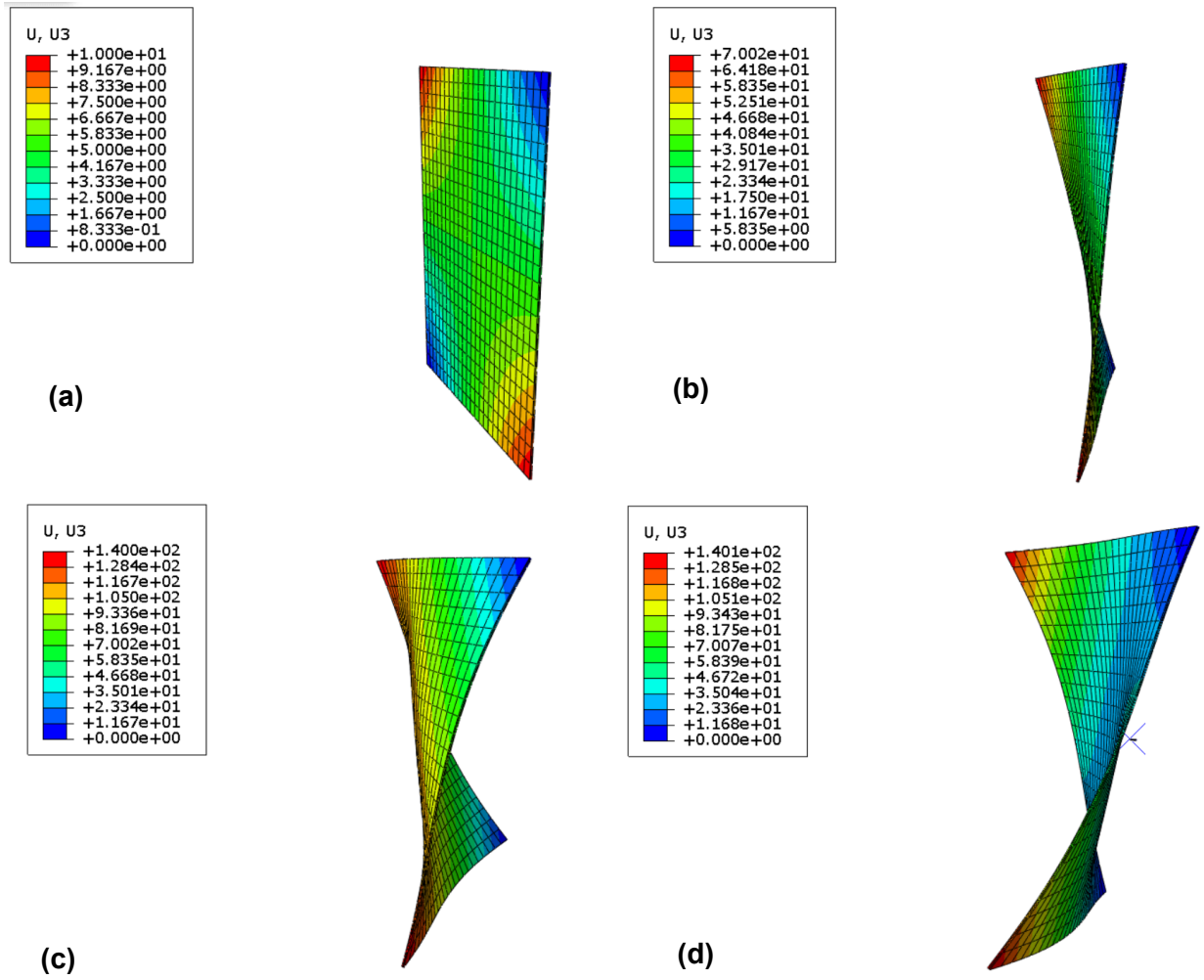

Fig. 9 – Deformed shape of the glass plate. Experiments and numerical model (scale factor 5): (a) corner displacement $\delta_{AC,z}$ = 10 mm; (b) at corner displacement $\delta_{AC,z}$ = 70 mm; (c) at corner

displacement $\delta_{AC,z}$ = 140 mm, undisturbed plate; (d) at corner displacement $\delta_{AC,z}$ = 140 mm, plate with disturbance

The maximum surface tensile stresses of the curved glass were calculated and found to be on the order of 45 MPa, far below the limit strength of heat tempered glass. This confirms that for slender plates like the one considered in the investigation the maximum curvature of glass panels that can be achieved with cold bending is restricted by the optical distortion induced by local instability of the panel.

4. Parametric analysis

Numerical analyses were performed using the finite element model presented in Section 3 with the aim of studying the influence of the size and shape of the glass plate on the cold bending procedure. Nine sizes of panels were studied (size in [mm]): five square plates, 1000 × 1000, 1500 ×1500, 2000 × 2000, 2500 × 2500, 3000×x 3000; and four rectangular plates, 2000 × 1000, 3000 × 1500, 3000 × 1000, 4500 × 1500. The aspect ratio μ, defined as the ratio of long to short edge lengths, varies from 1 to 3. For each panel the effect of thickness variation is evaluated by implementing three standard production thicknesses, namely 8, 10, and 12 mm.

The plate made of glass (properties: E = 70 GPa, ν = 0.22) is loaded at the four corners, the orientation is vertical and the static general analysis includes geometric non-linearity. The problem of a plate restrained at two opposite corners by pinned supports, and subjected to symmetric out-of-plane displacements $\delta_{AC,z}$ on the two other corners as sketched in Fig. 3 is considered in the analyses.

Out-of-plane displacement is imposed on points A and C (Fig. 3), and gradually increased until a ripple distortion of amplitude A_{dist} = 0.5 mm is produced on the stiffened diagonal .

For square plates Fig. 10a displays the buckling displacement δ_b*, conventionally defined as the maximum displacement that can be assigned on the forced corners to obtain a deviation from proportionality between centre and corner displacements ($\delta_{E,z} = \delta_{AC,z}/2$) less than 1%, and the maximum tensile stress of glass $\sigma_{t,max}$ at δ_b*.

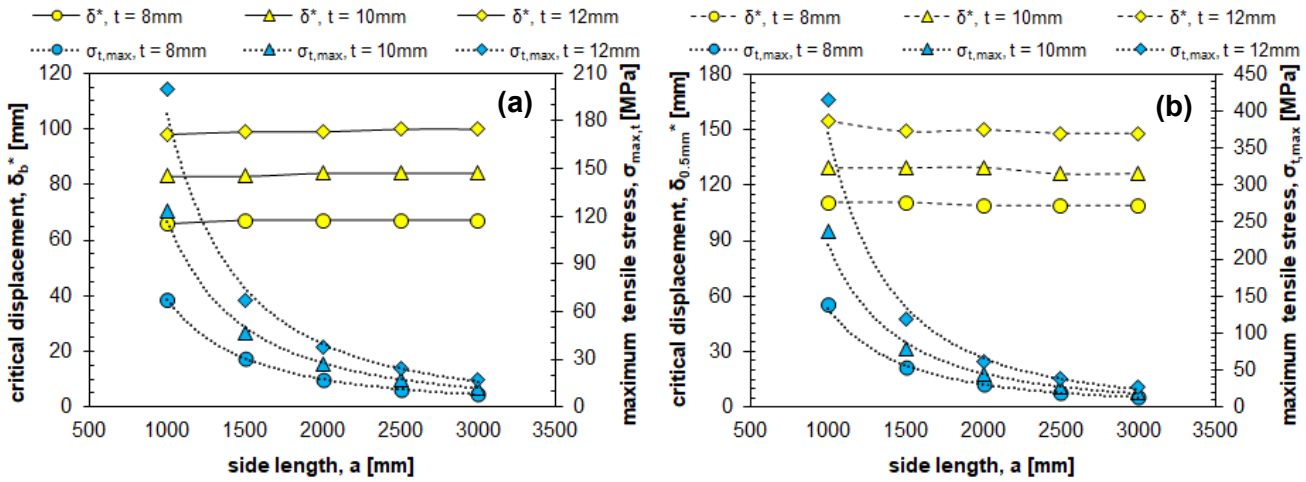

Fig. 10 – Cold bending of four-point loaded vertical square glass plates: (a) buckling displacement δ_b* and maximum tensile stress $\sigma_{t,max}$; (b) displacement $\delta_{0.5mm}$* at 0.5 mm ripple distortion, and maximum tensile stress $\sigma_{t,max}$

The buckling limit δ_b* is practically independent on the plate length, and depends on the glass thickness t only: the factor δ_b*/t counts 8.35, 8.36 and 8.27 for t = 8 mm, t = 10 mm, and t = 12 mm, respectively. This figure is close to the limit value δ_b*/t = 8.4 inferred [28] from Staaks' findings on plates loaded on one corner [18].

The maximum tensile stress of glass significantly decreases for increasing plate size and decreasing thickness. Actually, $\sigma_{t,max}$ depends on approximately power –2 of the edge length a , i.e. $\sigma_{t,max} = k_\sigma a^{-\beta}$, where β counts 1.96 for t = 8 mm, 2.09 for t = 10 mm, and 2.22 for t = 12 mm. It is noticed that for two panel sizes, namely 1000 x 1000 x 10 mm and 1000 x 1000 x 12 mm, the tensile stress exceeds 100 MPa, which can be assumed as a typical design strength of tempered glass [25].

The support reaction RFz at δ_b* was evaluated as well, though the relevant plots not reported. The force follows a similar trend to the surface stress, decreasing for slender plates according to a power relationship of type $RFz = k_{RF} a^{-\gamma}$, where γ counts 1.97 whichever the thickness.

However, from a practical point, until geometrical distortions impair the optical quality of the glass, bending of the glass plate can be extended beyond δ_b* without affecting the serviceability of the

panel. Fig. 10b displays, for square plates, the critical displacement $\delta_{0.5mm}$* which induces a distortion amplitude A_{dist} = 0.5 mm, and the relevant values of $\sigma_{t,max}$ at $\delta_{0.5mm}$*.

Like δ_b*, also $\delta_{0.5mm}$* is found to depend on the glass thickness, and be practically unaffected from the plate length: the factor $\delta_{0.5mm}$*/t counts 13.9, for t = 8 mm, and 12.9 for t = 10 mm and t = 12 mm, respectively (i.e., on average $\delta_{0.5mm}$*/t = 13.2).

The maximum tensile stress calculated at $\delta_{0.5mm}$* depends again on approximately power –2 of the side length a, i.e. $\sigma_{t,max} = k_\sigma\, a^{-\beta}$, where β counts 2.11 for t = 8 mm, 2.27 for t = 10 mm, and 2.45 for t = 12 mm. The assumed design strength of 100 MPa for tempered glass is exceeded from plates with size a = 1000 mm, whichever the thickness, and from plates with size a = 1500 mm and thickness of either t = 10 mm or t = 12 mm.

The reaction force at the support points increases too according to a power relationship of type $RFz = k_{RF}\, a^{-\gamma}$ with γ approximately 2 (range: 1.86 to 2.06). Such force must be taken into account for the design and selection of the restraints of the glass plate; moreover, the application of large forces may require the use of mechanical devices, with relevant increase in cost and complexity of the set-up.

Fig. 11 illustrates the effect of the aspect ratio μ of rectangular plates. Only the results relevant to the critical displacement $\delta_{0.5mm}$* are shown. Indeed, results for δ_b* replicated those found in a similar parametric research [44] on plates of same sizes and aspect ratios.

The critical displacement $\delta_{0.5mm}$* appears to be linearly dependent on both the glass thickness and the aspect ratio $\mu = b/a > 1$, and independent of the edge length a (Fig. 11a). The interpolation of all the results provided the following approximate expression

$$\delta_{0.5mm}^* = (2.4\,\mu + 10.7)\,t \qquad (1)$$

which is similar to the expression for the buckling limit of rectangular plates, namely $\delta_b^* = (1.5\,\mu + 6.9)\,t$, proposed by Galuppi [28].

The maximum tensile stress of rectangular plates is significantly lower than that of square plates (Figure 12b), decreasing by about 33% . for μ = 2 and by 39% for μ = 3, regardless of the glass

thickness. Equivalent results are found by analysing the decrease in the reaction force RFz (data not shown). For the considered rectangular plates the peak tensile stress limit of 100 MPa was never exceeded, whichever the thickness.

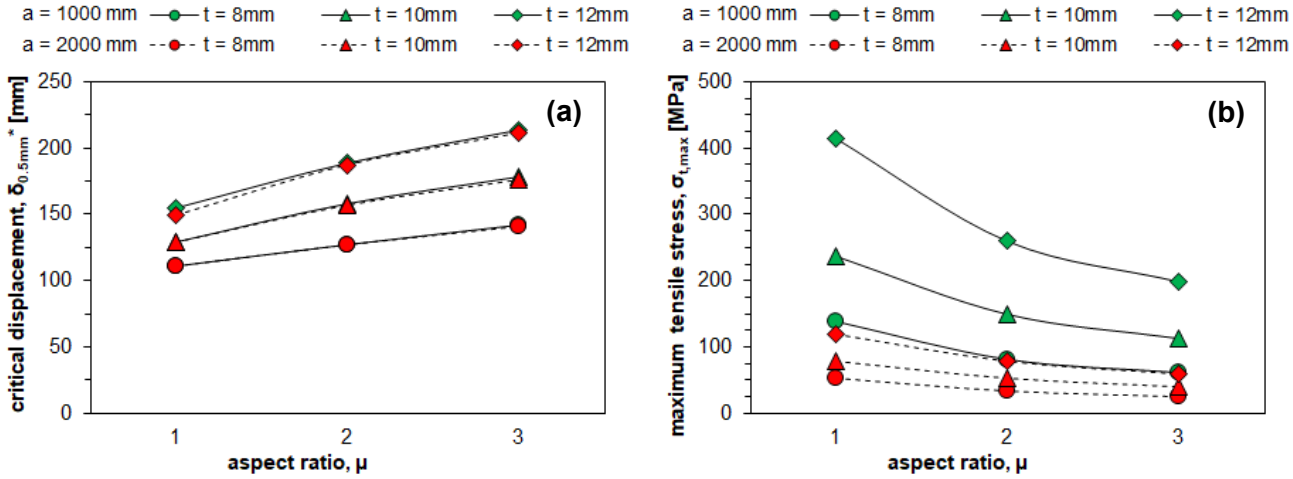

Fig. 11 – Cold bending of four-point loaded vertical glass plates of different aspect ratios μ: (a) displacement $\delta_{z,0.5mm}$* at 0.5 mm ripple distortion; (b) maximum tensile stress $\sigma_{t,max}$

5. Effect of wind load on curved glass plates

Additional analyses were performed to study the effect of an out-of-plane uniformly distributed load on double curved glass panes, simulating the effect of wind pressure on façade glazing units. Two studies were performed, considering either a symmetric or an asymmetric geometry of the bent plate, depending on the prescribed corner displacement during cold bending.

5.1 Symmetric plate geometry ($\delta_{AC,z} < \delta_b^*$)

The analyses are divided in two steps. In the first step, an out-of-plane displacement $\delta_{AC,z} = 8\ t < \delta_b^*$ is imposed on two opposite corners of the flat pane, while the displacements of the other two corners are restrained; rotations are left free . This way the plate is forced to deflect into a symmetric hyperparaboloid shape with deflection of the centre point $\delta_{E,z} = 0.5\ \delta_{AC,z}$. Once the desired shape is reached, the translation of forced corners is restrained too in any directions, simulating the fixing of the curved pane on a rigid frame through swivel supports. In the second step of the analysis the bent plate is subjected to the application of an increasing uniform pressure p normal to the original flat surface. Owing to the symmetry of the bent plate, the actual direction of the pressure is not significant. Fig. 12 displays the profiles of the diagonals of a 2000 × 2000 × 8 mm glass plate subjected to a prescribed displacement $\delta_{AC,z} = 64$ mm, at 0.1 kPa pressure increments . At the end of the warping, the deformed shape of the plate is symmetric, with a deflection of the centre point $\delta_{E,z} = 32$ mm. The pressure tends to increase the bending of the diagonal with “positive curvature” (i.e. with centre of curvature on the same side of the surface with respect to the applied pressure), and to decrease the bending of the other diagonal. The symmetry is lost, but the plate maintains it anticlastic geometry. However, at a pressure $p \approx 0.49$ kPa the second diagonal suddenly reverts its curvature towards the direction of the pressure, and the plate changes its geometry to synclastic. This sudden “jump” to a not adjacent equilibrium configuration, or “snap-through buckling”, can result in a sudden break of the glass plate, and therefore it is considered as an ultimate limit state condition. Notably, since the reversal of curvature is anticipated by the straightening of the diagonal, formation and growth of

ripples occurs along this diagonal before the snap-through is triggered; the distortion limit A_{dist} = 0.5 mm is exceeded at p ≈ 0.45 kPa.

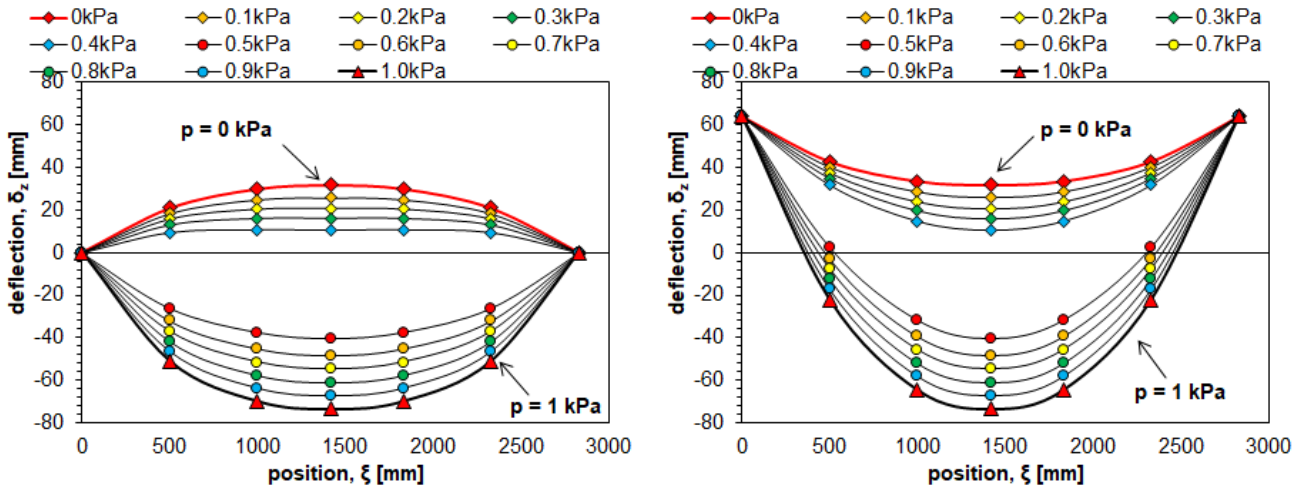

Fig. 12 – Diagonal profiles of a double curved symmetric glass plate subjected to pressure normal to its undeformed plane

Fig. 13 summarizes the occurrence of two phenomena, i.e. ripple growth and snap-through buckling, for curved square glass plates of different size and thickness. The 0.5 mm ripple amplitude is reached immediately before snap-through buckling is triggered, whichever the size of the plate. From a practical point, by assuming a reference value of 1 kPa for wind pressure [15] (solid horizontal line in Fig. 13), exposure to wind pressure can trigger an ultimate limit state for flexible plates: e.g., for plates with edge length a = 3000 mm, instability is triggered by critical pressures ranging from 0.1 kPa for t = 8 mm to 0.48 kPa for t = 12 mm. By reducing the size to a = 2000 mm, snap-trough buckling can occur below 1 kPa for thin plates only (t = 8 mm), while for smaller plates the limit pressure rises to unpractical levels.

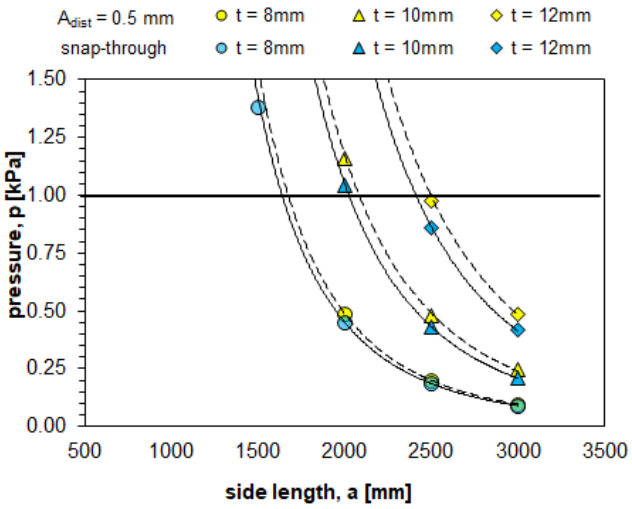

Fig. 13 – Response of symmetric double curved glass plates ($\delta_{AC,z} < \delta_b^*$): pressure levels inducing either 0.5 mm ripple distortion (A_{dist} = 0.5 mm) or snap-through buckling

5.2 Asymmetric plate geometry ($\delta_b^* < \delta_{AC,z} < \delta_{0.5mm}^*$)

The analyses are conducted in a similar way to Sec. 5.1, but in the first step the prescribed out-of-plane displacement is $\delta_b^* < \delta_{AC,z} = 0.75\ \delta_{0.5mm}^*$, hence forcing the plate to deflect into a double curved asymmetric shape. An increasing uniform pressure is then applied normal to the plate surface. However, since the deformed configuration is asymmetric, two analyses are performed, considering either the pressure applied in the same direction of the deflection of the centre point of the plate (case: *blow*) or in the contrary direction (case: *suction*).

The results for either loading condition are illustrated in Fig. 14. For clarity, only data points for $p \leq 1$ kPa are shown. Even in case of pressure applied on a plate deformed above δ_b^*, the onset of ripples on one diagonal and the achievement of the distortion limit A_{dist} = 0.5 mm anticipate the global instability of the plate; however, since the pressure levels triggering either phenomenon are very close each other, only the value relevant to snap-through instability is reported. The snap-through limit is slightly higher when the pressure is applied as *suction*; the influence of the pressure direction is greater for thicker plates, whereas for t = 8 mm it becomes negligible. As observed for the case of pressure acting on symmetrically deflected glazing, snap-through buckling is more likely to be

triggered in slender plates while it is deemed to be not a practical issue for rigid plates ($a \leq 1500$ mm or $a = 2000$ mm and $t \geq 10$ mm) since the critical pressure p is significantly higher than 1 kPa. Remarkably, snap-through buckling is engaged by higher pressure when the out-of-plane load is applied to plates deflected beyond the bifurcation point, because of a global stiffening effect introduced by the straightening of one diagonal and the onset of high membrane force along the other diagonal line that occur above δ_b*.

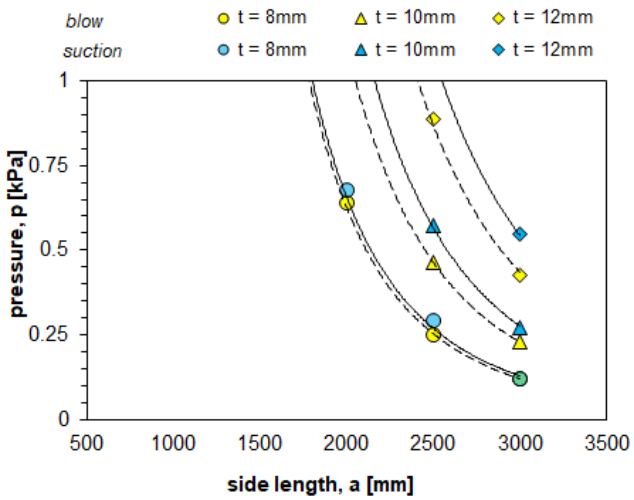

Fig. 14 – Response of asymmetric double curved glass plates (δ_b* < $\delta_{AC,z}$ < $\delta_{0.5mm}$*): pressure levels inducing snap-through buckling

6. Discussion and Conclusions

A fabrication method to obtain double curved glazing for free-form building façades is cold bending. With this technique, hyperbolic paraboloid surfaces can be obtained from flat glass panes by forcing their corners in out-of-plane directions. However, increasing the distortion may trigger an instability phenomenon: the plate develops an asymmetric deformed shape, in which the bending occurs mainly through one of the two diagonal lines. Deep research has been conducted in this field in the recent years, both experimentally and numerically [17-30].

The present research aims at providing more insight in this field, by tackling two subjects which have not been investigated in sufficient detail so far, namely the application of cold bending forming to vertically oriented panels, and the effect of wind pressure on vertical glass shells used in buildings as façade panels. The general case of a monolithic glass plate curved along two axes by forcing the displacements of two diagonally opposite corners while the other two corners are restrained by spherical joints is considered. The first part of the study addresses the behaviour of a vertical glass plate with realistic size subjected to cold bending.

The vertical orientation of the plate indeed decouples the bending process from the influence of the self-weight, and the glass unit initially develops a symmetric hyperparaboloid geometry where the two diagonal lines bend according to an almost parabolic shape and have the same curvature. However, for large distortions a new deformation mode is triggered, in which one diagonal stiffens and the second one becomes more curved. This form of buckling has been already studied and theoretical models have been developed to interpret the phenomenon [17]. Nevertheless, the experimental and numerical investigations carried out in the study allow to give more insight in this behaviour, highlighting two distinct deformation paths (Fig. 8):

- in ideally undisturbed conditions, after buckling has been triggered, the deformation increments are confined to the supported diagonal which keeps its parabolic shape, while the forced diagonal tends to straighten (Fig. 6 and Fig. 8);

- a mechanical disturbance, like e.g. a very small out-of-plane load, can pander the bent plate beyond its stability limit promoting a different deformation mode in which the support diagonal becomes stiffer and tends to return towards its original flat geometry, whereas the deformation of the plate is mainly accommodated by the deflection of the loaded diagonal (Fig. 7 and Fig. 9).

Hence it is argued that the vertical deflection of horizontally oriented glass plates due to the self-weight naturally drives the second deformation process, eventually leading to a buckling instability in which the stiffened diagonal reverts its curvature and that this behaviour can be eliminated by applying the cold bending process to vertical plates rather than horizontal, as already suggested by some Authors [25].

Interesting similarities can be found by comparing the results of the present study to those reported by Datsiou [25] for horizontal plates subjected to akin boundary conditions. Indeed, according to Fig. 5 in the reference, P- $\delta_{E,z}$ curves of horizontal plates with pinned supports at two corners resemble the *Ver*-disturbed plot in Fig. 4a of this study, with an initial linear relationship, followed by a second stage where the deflection of the centre point remains stationary, and a last stage with a gradual decrease of $\delta_{E,z}$. This backward movements of the centre of the plate is due to straightening of the supported diagonal noted above. What's different between the two situations is that, while in the horizontal plate the supported diagonal, initially deflected by the gravity, is straightened by forcing out-of-plane the other diagonal, in the vertical plate subjected to the disturbance the supported diagonal is smoothly deflected in the same direction of the imposed displacement until the bifurcation limit is reached, and changes its deformation mode only beyond this point.

It is also worth comparing the deflected shapes of the diagonal lines in vertical and horizontal plates. By referring to Fig. 7 in reference [25], it is noted that, in contrast to the symmetric curvatures of the two diagonals of the vertical plate before buckling (Figs. 6-9 in the paper), the geometry of the horizontal plate is never symmetric, and the shapes of the diagonals depart from each other as the load increases. In fact, the plate develops an initially deformed shape forced by gravity in which one of the two diagonals is more curved. Moreover, Datsiou [25] noticed that a particular form of snap-

though instability that is triggered when the out-of-plane loads on the two forced corner are applied in a direction opposite to the initial deflection induced by the self-weight of the plate. This phenomenon, which occurs in the early stages of bending, appears as a sudden change in the direction of curvature of both diagonals and can be result in breaking of the panel (see Fig. 14 in the reference [25]).

Eventually it must be recalled that the type of supports has a primary effect on determining the deformed shape of the plate. For example, replacing the pinned supports with as many roller supports at the extremities of the restrained diagonal forces the plate to bend approximately about a single axis, developing a cylindrical rather than a paraboloid surface [25, 26].

The critical value δ_b* of the corner displacement that triggers the buckling of vertical plates has been investigated in a parametric study performed using the validated numerical model (Fig. 10a). The thicker is the panel, the larger is the deflection than can be accommodated from the panel before instability is engaged, and a linear relationship exists between δ_b* and the plate thickness *t*, both for square and rectangular panels, as already noted [18-28].

Interestingly, similar results are found when the displacement $\delta_{0.5mm}$* that causes a geometrical distortion of the glass surface greater than 0.5 mm over 300 mm length, which has been proposed as a serviceability limit in order to control the optical distortion occurring in the curved glass plate [19, 32-33], is examined; results are shown in Fig. 10b for square plates, and Fig. 11a for rectangular plates. Based on this, a linear relationship between the displacement $\delta_{0.5mm}$*, which can indeed be considered to trigger a serviceability limit state failure of cold bent glass, and the thickness and aspect ratio of the glass unit has been proposed.

The maximum tensile stress attained on the surface extrados at either critical displacement has been evaluated too (Fig. 10a and Fig. 10b). Slender plates can be bent with a limited increase in the maximum tensile stress. On the contrary, cold forming of rigid plates causes a significant increase in surface tensile stresses. Thus, the thicker the plate, the larger will be the generated stress. The opposite trend is found regarding the aspect ratio: the higher μ, the lower the stress.

By taking into account a typical strength of tempered glass of 100 MPa, for stiff plates (i.e., with small size and/or high thickness) the limiting condition for cold bending of thick plates is dictated by the maximum stress that can be produced in glass, which can trigger an ultimate state failure, whereas for thin and flexible plates the limiting condition is dictated by the induced optical distortion of the plates (serviceability requirement). As shown in Fig. 11, in comparison to square plates, rectangular plates can accommodate larger deflections, and hence larger curvatures, without exceeding the limits on the distortion amplitude, or keeping the maximum tensile stress within reasonable levels. It must be indeed recalled that the stresses generated in the plate during cold bending represent permanent stresses that add up to the stresses induced by loads imposed on the glass during its service life, and must be taken into account for a safe design of the final construct.

In the second part of the study the effect of wind load on vertical glass panels in façades has been investigated numerically by applying a uniform pressure, acting almost perpendicular to the surface, to glass shells bent into an anticlastic shape. In comparison to previous experimental and numerical research on this subject [27, 36, 44] the novelties of the present study are: (i) the consideration of vertical plates, which allows to disregard the effect of gravity on the deformed shape of the plate, and (ii) the investigation of two different geometries, simulating plates warped either below the buckling limit, or above the buckling limit, but below the 0.5 mm distortion limit of the surface.

The analyses point out that the symmetric hyperparaboloid geometry developed below δ_b*, in which the centres of curvature of both diagonals lie on different sides of the panel surface, represents a metastable configuration in presence of the large plate deflections dictated by architectural requirements, and under the effect of an out-of-plane load, like e.g. the wind action, may suddenly buckle towards a new synclastic configuration, possibly producing the breaking of glass (Fig. 12). This can be an issue for slender plates, for which buckling may be triggered at pressures below the design value of 1 kPa (Fig. 13). It must be indeed remarked that the results provided by the study depend on the assumed boundary conditions for the glass units, and the use of more rigid clamps as proposed e.g. in [27, 36] can possibly shift the snap-through limit above safe levels.

Another finding of the study is that bending the glass plates beyond their buckling limit δ_b* into an asymmetric, approximately hyperparaboloid geometry may increase the stability against wind-induced buckling. By comparing the critical pressure calculated for asymmetrically versus symmetrically bent plates considered in the numerical analyses, the relevant ratio counts between 1.05 for t = 12 mm plates to more than 1.25 for t = 8 mm, suggesting that warping beyond δ_b* could be a practical way to increase the safety of thin plates which are more susceptible to wind pressure.

The present research has the merit of deepening some aspects of the instability of double curved glazing for free-form building façades, in particular as regards the effect of wind action, and is aimed at providing some suggestions for the practitioners who have the tackle the structural design of the glazing panels.

Future studies are required to evaluate the effects of different fixing conditions for the plate, as well as address cold bending of laminated glass panels, whose use is recommended for structural applications.

Acknowledgments

The Authors wish to thank Mr. Roberto Minerva and the Materials Testing Laboratory of Politecnico di Milano for making available the experimental facilities and for supporting the execution of the tests, and in particular Mr. Antonio Cocco and Mr. Marco Cucchi for their valuable help in the preparation of the set-up.

Funding

This research did not receive any specific grant from funding agencies in the public, commercial, or not-for-profit sectors.

References

[1] Eekhout M. Design, engineering, production & realisation of glass structures for ‘‘free-form” architecture. CWCT members meeting. Bath, United Kingdom, 2004.

[2] Neugebauer J. Applications for curved glass in buildings, J. Façade Design Eng (JDFE) 2014;2:67–83. https://doi.org/10.3233/FDE-150016.

[3] Teich M, Kloker S, Baumann H. Curved glass: bending and applications. In: Proc Engineered Transparency Conf; Germany; 2014. p. 75–83.

[4] Weber F. Curved glass structures. In: Proc glass performance days, Finland; 2009. p. 375–80.

[5] Von Starck A, Muhlbauer A, Kramer C. Handbook of thermoprocessing technologies, fundamentals, processes, components, safety. Vulkan-Verlag GMbH; 2005. p. 605–12.

[6] Saksala M. Curved and tempered glass – demand, challenge and opportunity for the market driven technology. In: Proc glass performance days, Finland; 2003. p. 63–5.

[9] Galuppi L, Royer-Carfagni G. Optimal cold bending of laminated glass. Int J Solids Struct 2015;67-68:231–43. https://doi.org/10.1016/j.ijsolstr.2015.04.023.

[8] Galuppi L, Royer-Carfagni G. Rheology of cold-lamination-bending for curved glazing. Eng Struct 2014;61:140–52. https://doi.org/10.1016/j.engstruct.2014.01.003.

[7] Galuppi L, Royer-Carfagni G. Cold-lamination-bending of glass: sinusoidal is better than circular. Compos B – Eng 2015;79:285–300. https://doi.org/10.1016/j.compositesb.2015.04.024.

[10] Abualnour M, Chikh A, Hebali H, Kaci A, Tounsi A, Bousahla AA, Tounsi A. Thermomechanical analysis of antisymmetric laminated reinforced composite plates using a new four variable trigonometric refined plate theory. Comput Concr 2019;24(6):489-98.

[11] Belbachir N, Draich K, Bousahla AA, Bourada M, Tounsi A, Mohammadimehr M. Bending analysis of anti-symmetric cross-ply laminated plates under nonlinear thermal and mechanical loadings. Steel Compos Struct 2019;33(1):913-24. https://doi.org/10.12989/scs.2019.33.1.081

[12] Bousahla AA, Mahmoud SR, Algarni A, Adda Bedia EA, Tounsi A. Buckling and dynamic behavior of the simply supported CNT-RC beams using an integral-first shear deformation theory. Comput Concr 2020;25(2):155-66.

[13] Sahla M, Saidi H, Draiche K, Bousahla AA, Bourada F, Tounsi A. Free vibration analysis of angle-ply laminated composite and soft core sandwich plates. Steel Compos Struct 2019;33(5):663-79. https://doi.org/10.12989/scs.2019.33.5.663

[14] Draiche K, Bousahla AA, Tounsi A, Alwabli AS, Tounsi A, Mahmoud SR. Static analysis of laminated reinforced composite plates using a simple first-order shear deformation theory. Comput Concr 2019;24(4):369-78.

[15] Fildhuth T, Knippers J. Double curved glass shells from cold bent glass laminates. In: Proc glass performance days, Finland; 2011. p. 384–9.

[16] Schittch C, Staib G, Balkow D, Schuler M, Sobek W. Detail: glass construction manual. Basel: Birkhäuser Verlag AG; 2007.

[17] Galuppi L, Massimiani S, Royer-Carfagni G. Buckling phenomena in double curved cold-bent glass. Int J Non-Linear Mech 2014;64:70–84. https://doi.org/10.1016/j.ijnonlinmec.2014.03.015.

[18] Staaks D. Cold bent glass sheets in blobs. University of Technology Eindhoven: MSc Thesis; 2003, in German.

[19] van Herwijen E, Staaks D, Eekhout M. Cold bent glass sheets in façade structures. Struct Eng Int 2004;14(2):98–101. https://doi.org/10.2749/101686604777964134.

[20] Eekhout M, Staaks D. Cold deformation of glass. In: Proc int symp application of architectural glass ISAAG, Germany; 2004.

[21] Eekhout M, Staaks D. Application of cold twisted temped glass panels in double curved architectural design, In: Proc glass performance days, Finland; 2007. p. 213–20.[22] Belis J, Inghelbrecht B, van Impe R, Callewaert D. Cold bending of laminated glass panels. HERON 2007;52(1/2):123–6. https://doi.org/10.1016/j.ijsolstr.2015.04.023.

[23] Belis J, Inghelbrecht B, van Impe R, Callewaert D. Experimental assessment of cold-bent glass panels. In: Proc glass performance days, Finland; 2007. p. 115–7.

[24] Mainil T. Exploratory investigation of the cold bending of thin glass. Ghent University: Master Thesis; 2015.

[25] Datsiou KC, Overend M. The mechanical response of cold bent monolithic glass plates during the bending process. Eng Struct 2016;117:575-90. https://doi.org/10.1016/j.engstruct.2016.03.019.

[26] Datsiou K. Design and Performance of Cold Bent Glass. PhD Thesis, University of Cambridge: PhD Thesis; 2017.

[27] Royer-Carfagni G, I. Iori I, Ferretti D, Franco A, Galuppi L, Manara, et al. Innovative steel glass composite structures for high-performance building skins (S+G). Final Report. Research for Coal and Steel (RFCS), Project RFSR-CT-2012-00026, European Union, 2017. https://doi.org/10.2777/312237.

[28] Galuppi L. Transformable curved thin glass greenhouse. Int J Struct Glass Adv Mat Res 2018;2:198-217. https://doi.org/10.3844/sgamrsp.2018.198.217.

[29] Nehring G, Siebert G. Design concept for cold bent shell structures made of thin glass. ce/papers, 2018;2(5-6):43-56.

[30] Spagnoli A, Brighenti R, Biancospino M, Rossi M, Roncella R. Geometrically non-linear bending of plates: Implications in curved building façades. Const. Build. Mat. 2019; 214:698-708. https://doi.org/10.1016/j.conbuildmat.2019.04.175.

[31] CEN (European Committee for Standardization). Glass in building. Thermally toughened soda lime silicate safety glass – Part 1: Definition and description. EN 12150-1:2000; 2000.

[32] Abbott A. Roller wave distortion. Definition, causes and a novel approach to accurate on-line measurement. In: Proc glass processing days, Finland; 2001. p. 226–30.

[33] Datsiou K, Overend M. Behaviour of cold bent glass plates during the shaping process. In: Proc engineered transparency int conf, Dusseldorf; 2014. p. 125–34.

[34] Helbig T, Kamp F, Schieber R, Oppe M, Torsing R, Kieft R. Double-layer curved steel-structure with bent glazing. New Departure Station Erasmusline, The Hague (NL). In: Bos F, Louter C, Belis J, editors. Challenging glass 5. Conference on architectural and structural applications of glass. Gent University; 2016.

[35] Lima-Castillo IF, Gómez-Martínez R, Pozos-Estrada A. Methodology to develop fragility curves of glass façades under wind-induced pressure. Int J Civ Eng 2019;17:347–59.

[36] Hoffmeister B, Di Biase P, Richter C, Feldmann M. Innovative steel-glass components for high-performance buildings skins: Testing of full-scale prototypes. Glass Struct Eng 2017;2:57-78. https://doi.org/10.1007/s40940-016-0034-1.

[37] CNR (National Research Council of Italy). Guide for the design, construction and control of buildings with structural glass elements. CNR-DT 210; 2013.

[38] Bennison SJ, Stelzer I. Structural properties of laminated glass, Short Course, In: Proc glass performance days, Finland; 2009.

[39] Galuppi L, Royer-Carfagni G. The effective thickness of laminated glass plates. J Mech Mat Struct 2012;7:375-400. https://doi.org/10.2140/jomms.2012.7.375.

[40] Galuppi L, Royer-Carfagni G. Effective thickness of laminated glass beams: new expression via a variational approach. Eng Struct 2012;38:53-67. https://doi.org/10.1016/j.engstruct.2011.12.039.

[41] Galuppi L, Royer-Carfagni G. The effective thickness of laminated glass: inconsistency of the formulation in a proposal of EN-standards. Compos Part B Eng 2013:55:109-18. https://doi.org/10.1016/j.compositesb.2013.05.025.[42] CEN (European Committee for Standardization). Glass in building. Thermally toughened soda lime silicate safety glass – Part 2: Evaluation of conformity/Product standard. EN 12150-2:2004; 2004.

[43] Abaqus/CAE 2017 Documentation. Analysis User's Manual, Simulia; 2017.

[44] Galuppi L, Di Biase P, Schaaf B, Richter C, Hoffmeister B, Feldmann M, Royer Carfagni G. Hybrid Steel-Glass cell: cold-twisting and buckling phenomena. In: Proc challenging glass conference 6 (CGC 6), Delft, The Netherlands; 2018. p. 217-28. https://doi.org/10.7480/cgc.6.2149.

[45] Beer B. Complex geometry facades – introducing a new design concept for cold-bent glass. In: Proc glass performance days, Finland; 2013. p. 516–22.